BIOCHEMISTRY
including biophysical chemistry & molecular biology

Article

pubs.acs.org/biochemistry

Amino Acid Determinants of Substrate Selectivity in the *Trypanosoma brucei* Sphingolipid Synthase Family

Michael A. Goren,[†,⊥] Brian G. Fox,[*,†,‡] and James D. Bangs[*,§]

[†]Department of Biochemistry, [‡]Transmembrane Protein Center, College of Agriculture and Life Sciences, and [§]Department of Medical Microbiology and Immunology, School of Medicine and Public Health, University of Wisconsin, Madison, Wisconsin 53706, United States

Supporting Information

ABSTRACT: The substrate selectivity of four *Trypanosoma brucei* sphingolipid synthases was examined. TbSLS1, an inositol phosphorylceramide (IPC) synthase, and TbSLS4, a bifunctional sphingomyelin (SM)/ethanolamine phosphorylceramide (EPC) synthase, were inactivated by Ala substitutions of a conserved triad of residues His210, His253, and Asp257 thought to form part of the active site. TbSLS4 also catalyzed the reverse reaction, production of ceramide from sphingomyelin, but none of the Ala substitutions of the catalytic triad in TbSLS4 were able to do so. Site-directed mutagenesis identified residues proximal to the conserved triad that were responsible for the discrimination between charge and size of the different head groups. For discrimination between anionic (phosphoinositol) and zwitterionic (phosphocholine, phosphoethanolamine) head groups, doubly mutated V172D/S252F TbSLS1 and D172V/F252S TbSLS3 showed reciprocal conversion between IPC and bifunctional SM/EPC synthases. For differentiation of zwitterionic headgroup size, N170A TbSLS1 and A170N/N187D TbSLS4 showed reciprocal conversion between EPC and bifunctional SM/EPC synthases. These studies provide a mapping of the SLS active site and demonstrate that differences in catalytic specificity of the *T. brucei* enzyme family are controlled by natural variations in as few as three residue positions.

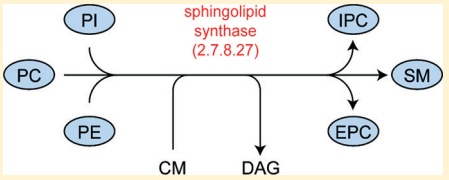

Sphingolipids (SLs) are ubiquitous in eukaryotes, where they are structural components of biological membranes, participate in protein sorting and cell signaling via membrane rafts, act as apoptotic and antiapoptotic secondary messengers, and serve as precursors for other essential lipid biosynthetic pathways like the Kennedy pathway.[1−6] Sphingolipid synthases (SLS) transfer a phosphoryl headgroup (Figure 1A) from phosphatidylinositol (PI), phosphatidylethanolamine (PE), or phosphatidylcholine (PC) to ceramide (CM) to generate inositol phosphorylceramide (IPC), ethanolamine phosphorylceramide (EPC), or sphingomyelin (SM) with release of diacylglycerol (DAG). These reactions can occur in the ER, Golgi, and the plasma membrane;[7,8] thus, trafficking of substrates and enzymes represents another important facet of sphingolipid biogenesis and function.[8−11]

Figure 1B shows a topology model for the SLS family, which is predicted to contain six transmembrane helices.[10,12] Sequence analyses revealed that conserved motifs of Ser, Gly, His (SGH) and His, Asp (H-X_3-D) originally identified in lipid phosphate phosphatases (LPPs), glucose-6-phosphatase, and other integral membrane phosphomonoester hydrolyzing enzymes[13] were also present in the mammalian sphingomyelin synthases (SMS),[10,14] fungal IPC synthase,[15] and the trypanosomal SLS family.[12] Collectively, these proteins comprise the phosphatidic acid phosphatase (PAP2) superfamily, PFAM Pf01569. In the following, the combination of His and Asp residues present in these motifs will be referred to as the HHD triad. Interestingly, chloroperoxidase also contains this motif[13,16] and thus provides a model for positioning of active site residues around a covalently bound phosphoryl group.[17]

The role of the HHD triad in catalysis was initially implicated by site-directed mutagenesis in the LPPs and later in the SMSs.[18] Transmembrane hidden Markov modeling[7,12,19] and biochemical fusion reporter studies[7,20,21] also suggested that the conserved motifs would be present in extramembrane loops, which were predicted to reside on the luminal side of the membrane bilayer.

Eukaryotic genomes typically contain multiple, highly conserved paralogs of SLS that allow the synthesis of a diverse array of sphingolipids.[7,22] For example, human sphingomyelin synthase 1 (hSMS1, UniProt Q86VZ5) is an SM synthase,[7] while hSMS2 (60% identity with hSMS1, UniProt Q8NHU3) is a bifunctional SM/EPC synthase[7,23] and hSMSr (34% identity with hSMS1, UniProt Q96LT4) is an EPC synthase.[21] Recently, we determined the enzymatic specificities of each of the set of four *Trypanosoma brucei* SLS paralogs, which have >90% primary sequence identity (Figure S1 of Supporting Information and ref 12). Among these, TbSLS1 is an IPC synthase and TbSLS2 is an EPC synthase, while TbSLS3 and TbSLS4 are bifunctional SM/EPC synthases.[24] The presence of the full suite of catalytic specificities in a single organism offers unique possibilities for studies of structure, function, and

Received: June 26, 2011
Revised: September 6, 2011
Published: September 7, 2011

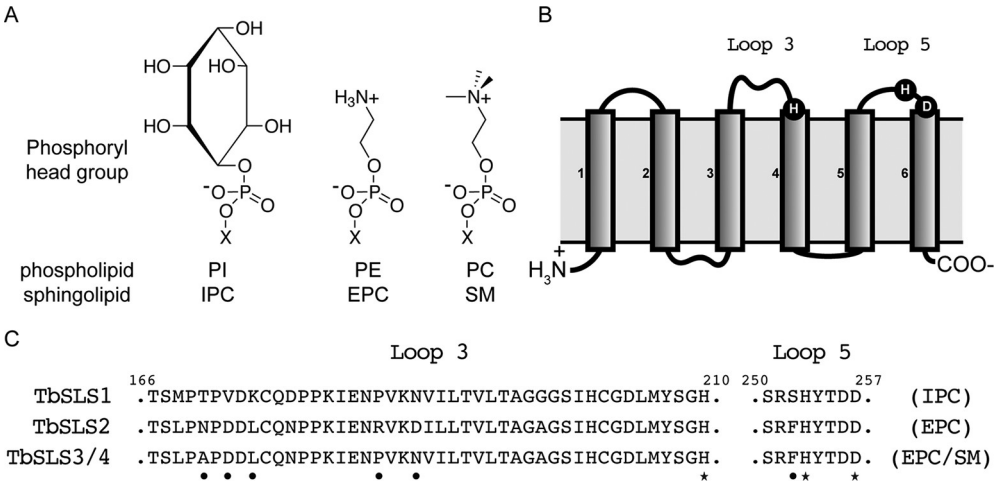

Figure 1. (A) Schematic of phospholipid head groups phosphorylinositol (PI), phosphotidylethanolamine (PE), and phosphotidylcholine (PC), which are transferred by SLS to ceramide (CM) yielding inositol phosphorylceramide (IPC), ethanolamine phosphorylceramide (EPC), and sphingomyelin (SM). X indicates the remainder of the phospholipid structure. (B) Diagram of the predicted topology of trypanosomatid SLSs adapted from ref 12. Transmembrane helices are numbered, and predicted positions of the proposed residues of the catalytic HHD triad (His210, His253, Asp257) are shown in the lumenal loops 3 and 5. (C) Alignment of the primary sequences of loops 3 and 5 from trypanosomatid SLSs as indicated. Stars indicate residues from the HHD triad, and black circles indicate other residues examined. The experimentally determined enzymatic activities of each paralog are shown at the right in parentheses.[24]

cellular physiology.[11,25] Upon consideration of the primary sequences of the enzymes from trypanosomes and other species, it is particularly striking that the marked discrimination between substrates by charge (PI vs PE/PC) and size of the headgroup (PI vs PE vs PC) must be provided by relatively few changes in residues (Figure 1C).

Efforts to study the mechanism of action and to identify the residues contributing to the selectivity observed in phosphosphingolipid synthesis have been generally hindered by issues arising in the production of integral membrane proteins for unambiguous functional analysis. For example, difficulties in establishing homologous transgenic lines, heterologous expression hosts, or in obtaining sufficient quantities of purified proteins for *in vitro* studies all constrained prior studies of the trypanosomal SLS paralogs. To overcome the latter limitation, we utilized a cell-free translation system developed for the translation and purification of integral membrane proteins.[24,26] This approach facilitated the analysis of mutations in the TbSLS family. From this work, the requirement for the HHD triad in catalysis has been established in the trypanosomal SLS family. Moreover, three residues in the sequences proximal to the HHD triad are shown to have an essential role in establishing substrate selectivity in the entire *T. brucei* SLS family. The role of these residues in substrate-specific reaction mechanisms is proposed, and similarities and differences of the trypanosomal SLS with the broader family of SLS and their relationship to the larger PAP2 superfamily are discussed.

MATERIALS AND METHODS

Materials. Unless otherwise stated, bacterial growth reagents, antibiotics, routine laboratory chemicals, and disposable labware were from Sigma-Aldrich (St. Louis, MO), Fisher (Pittsburgh PA), or other major distributors. DNA sequencing was performed in the University of Wisconsin Biotechnology Center.

Cloning. TbSLS open reading frames (ORFs) were amplified[24] by PCR using PfuUltra II DNA polymerase (Stratagene, San Diego, CA) and specific primers containing 5′ SgfI and 3′ PmeI sites prior to cloning into the pEU-C-His Flexi plasmid.[27,28] pEU-C-His Flexi is available from the NIH Protein Structure Initiative Materials Repository (http://psimr.asu.edu/). The specific nucleotides of the trypanosomatid SLS ORFs and their TryTrp and UniProt database accession numbers are *TbSLS1*, nt 1−1011, Tb09.211.1030, Q38E53; *TbSLS2*, nt 1−969, Tb09.211.1020, Q38E54; *TbSLS3*, nt 1−987, Tb09.211.1010, Q38E55; *TbSLS4*, 1−1041, Tb09.211.1000, Q38E56. *T. brucei* SLS genes were amplified from Lister 427 strain genomic DNA. All PCR-amplified genes were sequence verified. Plasmid DNA for transcription reactions was purified using Marligen maxi-prep kits (Marligen Biosciences, Ijamsville, MD).

Site-Specific Mutagenesis. Mutagenesis was performed using either the PCR-based QuikChange Multi Site-directed mutagenesis kit (Stratagene, San Diego, CA) as described previously[24] or by using a two-step overlap extension PCR. For the latter, the first step consisted of two reactions: the first reaction contained a *TbSLS* paralog specific 5′ primer containing an SgfI restriction site and an ∼35 bp mutagenic 3′ primer centered at desired codon; for the second reaction a complementary mutagenic 5′ primer and a *TbSLS* paralog specific 3′ primer containing a PmeI restriction site were used. In the second overlap extension PCR step, 5 μL from each of the aforementioned PCR reactions was used as the template and amplified using the appropriate *TbSLS* paralog specific 5′ and 3′ primers. Mutagenic primer sequences are presented in Table S1 of the Supporting Information. All mutagenized *TbSLS* constructs were sequence verified by work carried out at the University of Wisconsin Biotechnology Center.

Liposome Preparation. Unilamellar liposomes (100 nm) were prepared using an Avanti miniextruder and soybean total lipid extract [soy PC, 20%, catalog no. 541601G, Avanti Polar Lipids, Alabaster, AL, containing (wt/wt %) 24.0% PC, 18.6% PE, 11.5% PI, 4.3% PA, 4.6% lyso-PC, and 37.0% unknown]. Lipid powder dissolved in chloroform was dried and rehydrated with 25 mM HEPES, pH 7.5, containing 100 mM NaCl at a concentration of 15 mg/mL.[26,29] The solution was vortexed, subjected to three freeze−thaw cycles, and extruded in an Avanti miniextruder by 11 passes through 400 nm track-etch polycarbonate membranes followed by 100 nm track-etch

polycarbonate membranes (Nucleopore, Pleasanton, CA). Liposomes were stored at −80 °C.

In Vitro Transcription and Translation. These were performed by a modification of a previously described protocol.[29] For each translation reaction, 10 μL of transcription reaction was prepared containing 0.8 μg of plasmid DNA, transcription buffer (80 mM HEPES-KOH, pH 7.8, containing 20 mM magnesium acetate, 2 mM spermidine hydrochloride, and 10 mM DTT), 4 mM of each nucleotide triphosphate (ATP, GTP, CTP, and UTP), 3.2 unit/μL SP6 RNA polymerase, and 1.6 U/μL RNasin (each from Promega, Madison, WI). After a 5 h incubation at 37 °C, the transcription reaction was transferred to a 12 kDa MWCO dialysis cup (Cosmo Bio, Tokyo, Japan) containing 15 μL of WEPRO 2240 wheat germ extract (Cell Free Sciences, Yokohama, Japan), 12.5 μL of 2× translation buffer with amino acids (60 mM HEPES-KOH, pH 7.8 containing 200 mM potassium acetate, 5 mM magnesium acetate, 0.8 mM spermidine hydrochloride, 8 mM DTT, 2.4 mM ATP, 0.5 mM GTP, 32 mM creatine phosphate, 0.01% (w/v) sodium azide and 0.6 mM of each amino acid), 35.6 μg creatine kinase (Roche Applied Science, Indianapolis, IN, Louisville, KY), 60 μg of soy liposome, and deionized water to 40 μL. The dialysis reaction was suspended in 1× translation buffer and incubated at 26 °C overnight. Proteoliposomes were recovered from two pooled translation reactions by density gradient floatation, and the yield of the translation product was estimated using the Criterion Stain-Free gel imaging system (Bio-Rad, Hercules, CA) and known amounts of creatine kinase as the protein standard. Proteoliposomes were stored at −20 °C.

Sphingolipid Synthesis Assay. Each TbSLS translation product (5 μg of protein as determined by stain-free imaging) was incubated with 2.5 μM NBD-C6-CM (6-((*N*-(7-nitrobenz-2-oxa-1,3-diazol-4-yl)amino)hexanoyl)sphingosine, Invitrogen, Molecular Probes) in 50 mM MES, pH 6.5, 50 mM NaCl, 5 mM KCl, 1 mM EDTA at 30 °C for 2.5 h as previously described.[24] Proteoliposomes provided phospholipids needed for reaction. Reactions were terminated by addition of 200 μL of distilled H_2O followed by 2.0 mL of chloroform:methanol (1:1 v/v) and mixed. Insoluble material was removed by centrifugation, the organic layer was dried under N_2, and the desiccated lipids were partitioned in *n*-butanol/water. The *n*-butanol phase was recovered and fractionated by thin-layer chromatography in chloroform:methanol:acetic acid:water (25:15:4:2 v/v/v/v) on TLC silica gel 60 plates (Merck KGaA, Darmstadt, Germany). Fluorescent lipids were visualized on a Typhoon 9410 (GE Healthcare, Little Chalfont, Buckinghamshire, UK) imaging system with ImageQuant software. Fluorescence intensity comparisons are valid within individual plates only. The assignments of NBD-C6 derivatives of SM, IPC, and EPC were based on mobility standards or inferred by relative mobility.[12] For study of the reverse reaction, resulting in the formation of NBD-C6-CM, 5 μg of TbSLS translation product was assayed as above except with the substitution of 2.5 μM of BSA-stabilized NBD-C6-SM (6-((*N*-(7-nitrobenz-2-oxa-1,3-diazol-4-yl)amino)hexanoyl)-sphingosylphosphocholine, Invitrogen) for NBD-C6-CM. BSA stabilization was performed as previously described.[30] Wheat germ extract contributed diacylglycerol to the proteoliposomes as needed for studies of the reverse reaction. Reactions were terminated and processed as above and fractionated by thin-layer chromatography in chloroform:methanol:ammonium hydroxide (65:25:4) and imaged as above.

Bioinformatics. Related proteins were recovered from the UniProt web portal[31] by using BLAST and the complete TbSLS4 protein sequence as the query. The top 250 sequences ranked according to increasing *e*-values were examined. Redundant sequences were eliminated from further analysis along with those sequences that lacked residues from the HHD triad, were shorter than 200 or longer than 700 residues, or had extensive tracks of repetitive sequences (e.g., Q, P, or S/T). From the 250 sequences, 43 were eliminated by these criteria. Sequence alignments were performed using ClustalW[32] as implemented in MegAlign v.9.04 (DNAStar, Madison, WI). Phylogenetic trees were generated with 1000 trials of bootstrap recalculation using a random seed of 111. Precalculated homology models were obtained at the Protein Structure Initiative Protein Model Portal Web site (http://www.proteinmodelportal.org/).[33]

RESULTS

Catalytic HHD Triad in TbSLSs. In order to test whether the HHD triad was involved in TbSLS catalysis, Ala substitutions of H210, H253, and D257 in TbSLS1 (IPC synthase) and TbSLS4 (SM/EPC synthase) were prepared (Figure 1C). The wild-type and single Ala mutations of the TbSLS paralogs were produced individually in the cell-free translation system supplemented with unilamellar liposomes and the proteoliposomes were purified by gradient centrifugation.[29] SDS-PAGE of the purified proteoliposomes indicated that each TbSLS variant was associated with the lipid fraction and synthesized to similar levels (Figure 2A shows results for TbSLS4). The protein expression level observed for the

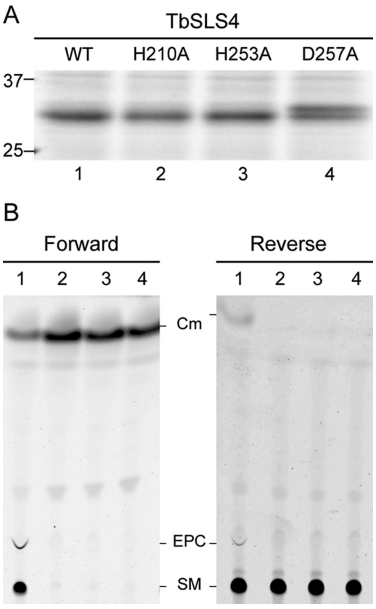

Figure 2. Catalysis by TbSLS4 HHD triad mutations. (A) Translation and proteoliposome purification of TbSLS4 and variants with Ala mutations in the HHD triad shown by SDS-PAGE. The positions of molecular mass standards (kDa) are indicated. BioRad stain-free analysis was used to normalize the amount of TbSLS from these preparations to be used in enzyme reactions. (B) Thin-layer chromatography fractionation of products from reactions containing either NBD-C6-CM (left panel) or NBD-C6-SM (right panel) and ~5 μg of TbSLS4 or variants with the indicated Ala mutations of the HHD triad. The migration positions of SM and CM were determined from mobility standards, while EPC migration was based on comparison to the known second product of TbSLS2.

different variants ranged from 0.2 to 0.5 mg/mL of reaction, and the purity of the proteoliposomes was comparable to that shown previously.[24]

The enzymatic activity of each mutated enzyme was determined in the standard sphingolipid synthesis assay using normalized amounts of protein. Control reactions showed that the wheat germ extract alone did not catalyze any phosphoryl transfer reactions with the NBD-labeled substrates. While wild-type TbSLS4 synthesized both NBD-C6-SM and NBD-C6-EPC as previously observed,[24] the three TbSLS4 variants with Ala mutations in the HHD triad had no detectable activity (Figure 2B, left panel). Likewise, wild-type TbSLS1 synthesized NBD-C6-IPC, while the three TbSLS1 variants with Ala mutations in the HHD triad were not active (data not shown). Additionally, TbSLS4 synthesized detectable amounts of NBD-C6-CM and NBD-C6-EPC when NBD-C6-SM was substituted for NBD-C6-CM as the fluorogenic substrate in the standard assay conditions, demonstrating the reversibility of the phosphoryl transfer reaction as previously shown for human SMSs.[7] The observed incorporation of NBD into NBD-C6-EPC (Figure 2B, right panel) most likely represented secondary synthesis by the forward reaction once sufficient NBD-C6-CM accumulated. None of the TbSLS4 variants with Ala mutations were active in the reverse reaction. In combination, these results demonstrate that the HHD catalytic triad has an essential role in SLS catalysis.

Determinants of Substrate Selectivity. The primary sequences of the four TbSLS paralogs have >90% identity, and this exceeds 95% when the variable C-terminal cytoplasmic domain and conservative substitutions in the transmembrane helices are not included in the alignment analysis.[12] This leaves few residues positions that may account for the observed differences in substrate selectivity. Notably, the majority of the residue differences are located adjacent to the residues of the HHD triad in loops 3 and 5 (Figure 1C and Figure S1).

To better understand the origin of the observed selectivity for zwitterionic head groups in the SM/EPC synthases (substrates PC and PE, Figure 1A) versus an anionic headgroup in the IPC synthase (substrate PI, Figure 1A), the non-conserved residues in loops 3 and 5 were aligned and correlated with either PC/PE or PI production. This analysis revealed four residues in loop 3 that were varied. Among these four, D172 was intriguing as it was the only negatively charged residue among the nonconserved residues in both TbSLS3 and TbSLS4 and thus might contribute to a preferential recognition of positively charged head groups instead of an anionic headgroup. In addition, the single nonconserved position in loop 5, present as either F252 or S252, was previously associated with production of either SM/EPC or IPC, respectively.[24]

To test the possible role of these residues in substrate selectivity, reciprocal mutations at positions 172 and 252 were introduced either individually or in tandem and the mutated forms of TbSLS1 and TbSLS3 were then produced in the cell-free system. As judged by stain-free SDS-PAGE, all TbSLS1 and TbSLS3 variants were translated and were purified as proteoliposomes by density gradient centrifugation (Figure 3A). Normalized amounts of the TbSLS variants were tested in the standard SLS synthesis assays.

V172D TbSLS1 was a trifunctional enzyme, with newly introduced SM/EPC synthetic activity concomitant with retention of IPC synthesis at a level comparable to the wild-type TbSLS1 (Figure 3B, lanes 1 and 2). In contrast, D172V TbSLS3 was inactive (Figure 3B, lanes 5 and 6). As reported previously,[24] singly mutated S252F TbSLS1 showed reduced IPC synthesis

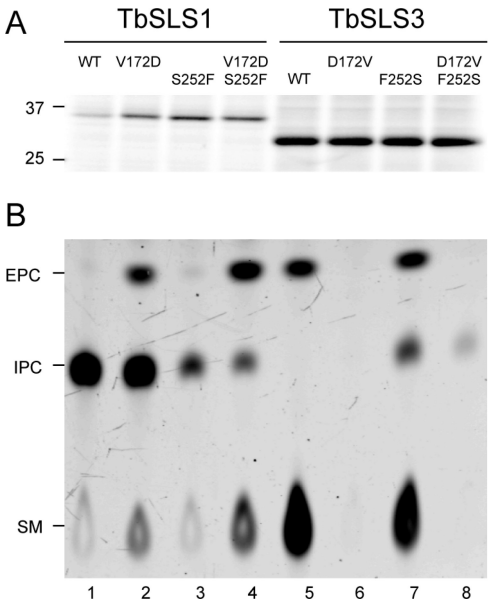

Figure 3. Residues involved in conversion between IPC and SM/EPC synthase activity. (A) SDS-PAGE analysis of proteoliposomes containing the indicated TbSLS variant. The positions of molecular mass standards (kDa) are indicated. (B) Thin-layer chromatography analysis of products from standard synthase assays of proteoliposomes containing ~5 μg of TbSLS or the indicated mutated variants and NBD-C6-CM. The mobility positions of different products are indicated.

(Figure 3B, lanes 1 and 3), whereas the reciprocal F252S TbSLS3 became a bifunctional enzyme, with enhanced IPC synthesis and minimal impact on SM/EPC synthesis (Figure 3B, lanes 5 and 7).

The doubly mutated V172D/S252F TbSLS1 was also trifunctional and showed enhanced SM/EPC synthesis but greatly diminished IPC synthesis (Figure 3B, lanes 1 and 4). The reciprocal D172V/F252S TbSLS3 had no detectable SM/EPC synthesis activity, but was a modestly active IPC synthase (Figure 3B, lanes 5 and 8). Although not shown, mutagenesis of TbSLS4 yielded product distributions similar to those observed with TbSLS3, which is consistent with the high sequence identity of these two paralogs (98% identical over 250 residues encompassing the active site and transmembrane helices). These results indicate that residues at positions 172 and 252 are important in determining the substrate selectivity.

We also investigated position 174 in loop 3, as K174 in TbSLS1 might place a positive charge in the active site that could destabilize PC/PE binding if this residue were introduced into TbSLS3. Either alone or in combination with mutations at residues 172 or 252, reciprocal mutations at residue 174 did not noticeably alter product distributions compared to the wild-type enzymes or those with single, or double mutations in both TbSLS1 and TbSLS3 (data not shown). However, Figure 4 shows that triple mutations involving residues 172/174/252 further modified the selectivity for the nonionic PI headgroup as compared to the 172/252 double mutations. Thus, D172V/L174K/F252S TbSLS3 had enhanced IPC synthesis compared to D172V/F252S TbSLS3 (Figure 4B, lanes 4–6), while the reciprocal mutations in TbSLS1 further decreased IPC synthesis (Figure 4B, lanes 1–3).

Through their respective preferences for production of either EPC or SM, TbSLS2 and TbSLS4 must also discriminate between the smaller primary amine headgroup of PE and the larger

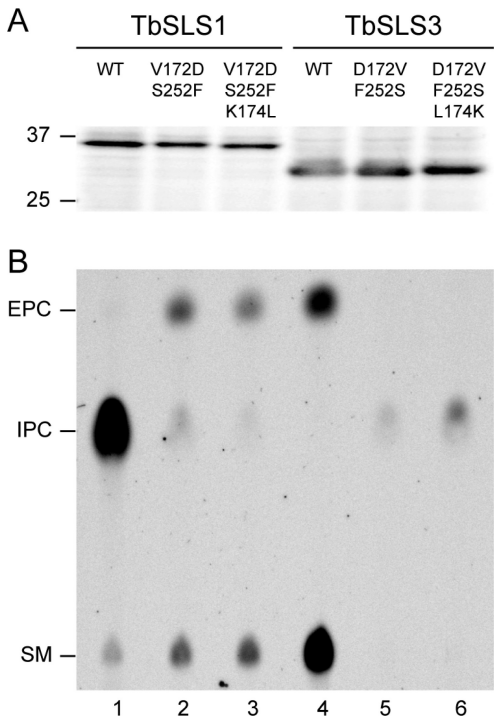

Figure 4. Reciprocal mutations leading to conversion between IPC and SM/EPC synthase activity in TbSLS1 and TbSLS3. (A) SDS-PAGE analysis of expression for the different TbSLS variants with mutations indicated. (B) Thin-layer chromatography analysis of products given by the different TbSLS variants using NBD-C6-CM as substrate. Three mutations convert TbSLS1 from an IPC synthase to a predominantly bifunctional SM/EPC synthase. The reciprocal mutations convert TbSLS3 from a bifunctional SM/EPC synthase into an IPC synthase.

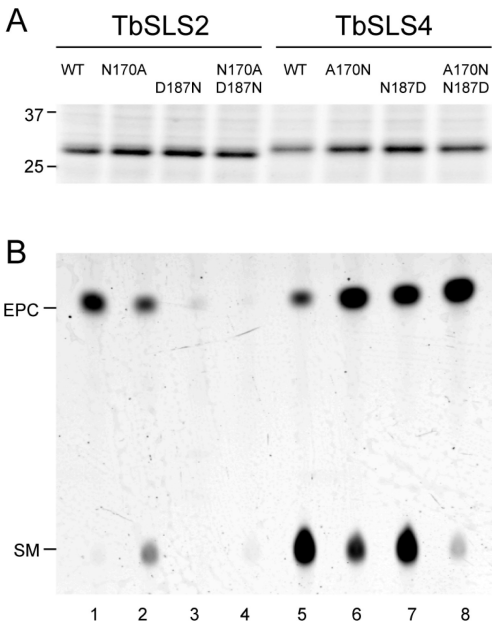

Figure 5. Reciprocal mutations leading to conversion between monofunctional EPC and bifunctional SM/EPC reactions in TbSLS2 and TbSLS4. (A) SDS-PAGE analysis of expression for the different TbSLS variants with mutations indicated. (B) TLC analysis of products given by the different TbSLS variants using NBD-C6-CM as substrate. One mutation converts TbSLS2 from an EPC synthase to a bifunctional SM/EPC synthase. Additional mutations inactivate TbSLS2. Two reciprocal mutations convert TbSLS4 from a bifunctional SM/EPC synthase into an EPC synthase.

quaternary amine headgroup of PC. There are three nonconserved positions in loop 3 of TbSLS2 and TbSLS4 with either size or polarity differences for their side chains: 170 (Asn vs Ala), 184 (Arg vs Pro), and 187 (Asp vs Asn). Single, double, and triple mutations at these positions were created by site-directed mutagenesis, expressed, purified as proteoliposomes, and tested in the standard assay. Figure 5 shows results of single and double reciprocal mutations, while Figure S2 shows other mutagenesis results. The mutation N170A converted TbSLS2 from an EPC synthase to a bifunctional SM/EPC synthase, but additional mutations inactivated TbSLS2. Two reciprocal mutations converted TbSLS4 from a bifunctional SM/EPC synthase into an EPC synthase. As single mutations at positions 170, 184, and 187 in TbSLS2 and TbSLS4 modestly influenced the partition between SM and EPC synthesis, we also investigated double (Figure 5) and triple (Figure S3) mutations at these combinations. However, these did not further alter the product distributions.

■ DISCUSSION

Owing to the importance of sphingolipids in eukaryotes, there are numerous genes now annotated to encode enzymes responsible for their synthesis.[10] Since these are integral membrane enzymes, it has been difficult to experimentally evaluate how these proteins might direct the selective use of substrate polar head groups in order to yield the diverse set of phosphosphingolipid products. Recently, we demonstrated that wheat germ cell-free translation could be used to generate functional TbSLS enzymes and discerned their separate enzymatic functions as defined by their unique product distributions.[24]

In this work, we deduced by sequence alignments a set of residue positions in the TbSLS family that might be involved in substrate selectivity and then used site-directed mutagenesis and cell-free translation to experimentally probe these deductions. Our results show that the HHD triad identified in the phylogenetically related LPP and the SMS families is also critical for enzymatic activity in the trypanosomal SLS clade.[7,22] Furthermore, nonconserved residues adjacent to the HHD triad were correlated with changes in reaction products, providing new insight into how the trypanosomal SLSs recognize different classes of substrates delineated by the charge and size of their head groups.

Consensus Active Sites for Different Sphingolipid Synthases. The experimentally determined activities for trypanosomatid SLS proteins[12,24,34] and the mutagenesis studies presented here demonstrate that residues in loops 3 and 5 are important determinants of the catalytic specificity. Figure 6A shows that all kinetoplastid IPC synthases have a Ser residue at position 252, either Val or Asp at position 172 and either Lys or His at position 174. Correspondingly, F252S TbSLS3 acquired partial ability to produce IPC, and D172V/L174K/F252S TbSLS3 produced only IPC, albeit with a decrease in total product yield relative to TbSLS3 (Figure 4). Figure 6A also shows that the EPC synthases have Asn at position 170, while SM/EPC synthases have Ala at this position and IPC synthases have either Ala or Thr. Correspondingly, N170A TbSLS2 acquired ability to produce both EPC and SM (Figure 5). Furthermore, Figure 6A shows that SM/EPC synthases have Ala at position 170 and Asn at position 187, while EPC synthases have Asn at position 170 and Asp at

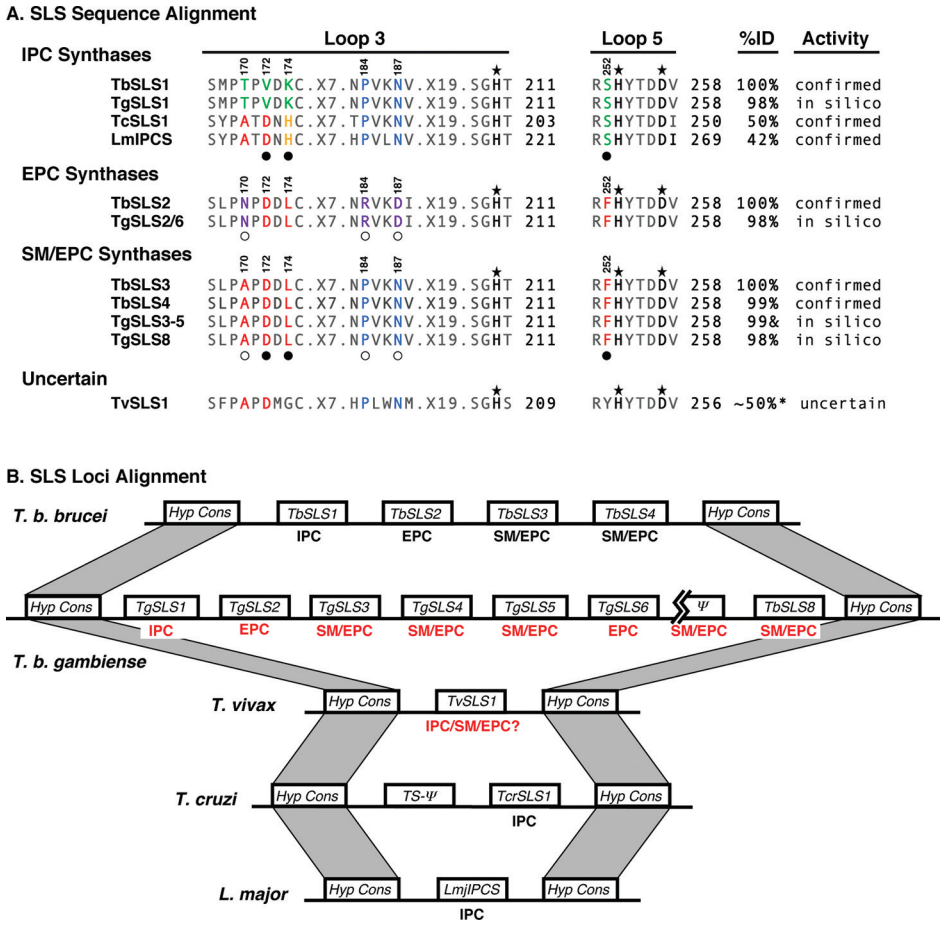

Figure 6. Alignment of the syntenic SLS loci in kinetoplastid protozoa. (A) Sequence alignments of the kinetoplastid SLS orfs in the regions of loop 3 and loop 5 according to experimentally determined catalytic activity classes of the *T. b. brucei* enzymes. All sequences are aligned to the corresponding experimentally defined Lister Strain 427 TbSLSs (top in each case). Residues that were subject to experimental mutation as described in the text are numbered. Closed circles: reciprocal mutation between TbSLS1 and TbSLS3. Open circles: reciprocal mutation between TbSLS2 and TbSLS4. Stars indicate the HDD triad (black). Red: conserved SM/EPC synthase residues. Green: conserved IPC synthase residues. Blue: shared SM/EPC and IPC synthase residues. Purple: unique EPC synthase residues. Yellow: unique LmjIPCS and TcSLS1 residues. Percent identity (%ID) within each activity class relative to the TbSLS type sequence is indicated. Divergent C-terminal amino acid sequences following the last common residue (TbSLS1−4, N296) were deleted for generation of the identity matrix. Experimentally confirmed and in silico activities are indicated. TbSLS sequence conservation between different activity classes was ~90% in all cases. *T. vivax* SLS1 identity versus all TbSLS activity groups was ~50%. (B) Alignment of the SLS loci from the assembled kinetoplastid genomes. Flanking orthologous conserved hypothetical genes set the common boundary for each locus. Experimentally confirmed SLS activities are denoted in black below each orf. Predicted activities based on loops 3 and 5 are indicated in red. Note that *TgSLS7* of the *T. b. gambiense* locus is a pseudogene, and the *T. cruzi* locus contains an inserted trans-sialidase (TS) pseudogene. (A, B) TriTryp database accession numbers are *T. b. brucei*, TbSLS1−4, Tb427tmp.211.1000-Tb427tmp.211.1030; *T. b. gambiense*, TgSLS1−8, Tbg972.9.5370-Tbg972.9.5300; *T. cruzi*, TcSLS1, Tc00.1047053506885.124; *T. vivax*, TvSLS1, TvY486_0904020; *L. major*, LmIPCS, LmjF35.4990.

position 187. Correspondingly, A170N/N187D TbSLS4 was exclusively converted to an EPC synthase (Figure 5).

The specific molecular interactions that define how the above residues contribute to the substrate selectivity in the trypanosomal SLS family cannot be assigned from this work. It is also clear that reciprocal mutations among closely related orthologs did not always lead to fully reciprocal changes, indicating that additional subtle features contribute to the reaction specificity of these enyzmes. Nevertheless, the work presented here demonstrates the importance of the HHD motif in catalysis and also identifies nonconserved residue positions near to this motif that profoundly influence the product distributions. This provides a new expanded view of the composition of the SLS active site.

Sequence Alignments with Other Trypanosomal SLS. The residues in these loops were used for in silico prediction of the catalytic specificity of closely related trypanosomatid SLSs (Figure 6A) including the African trypanosomes *T. b. brucei*, *T. b. gambiense*, and *T. vivax*, the South American trypanosome *T. cruzi*, and the old world leishmania, *L. major* [tritrypdb.org[35]]. These genomes collectively harbor 14 SLSs orthologues whose overall sequence identity placed them into three catalytic specificity groups.

The extension of this analysis to the mammalian SLS clade is complicated by the lack of conservation near to the SGH and HX_3D motif residues, insertions in the sequence relative to the loops 3 and 5 from the trypanosomal proteins, and also by lesser number of experimentally verified functions within the mammalian clade, so this analysis was not undertaken. However, it would be interesting to learn whether the cell-free translation

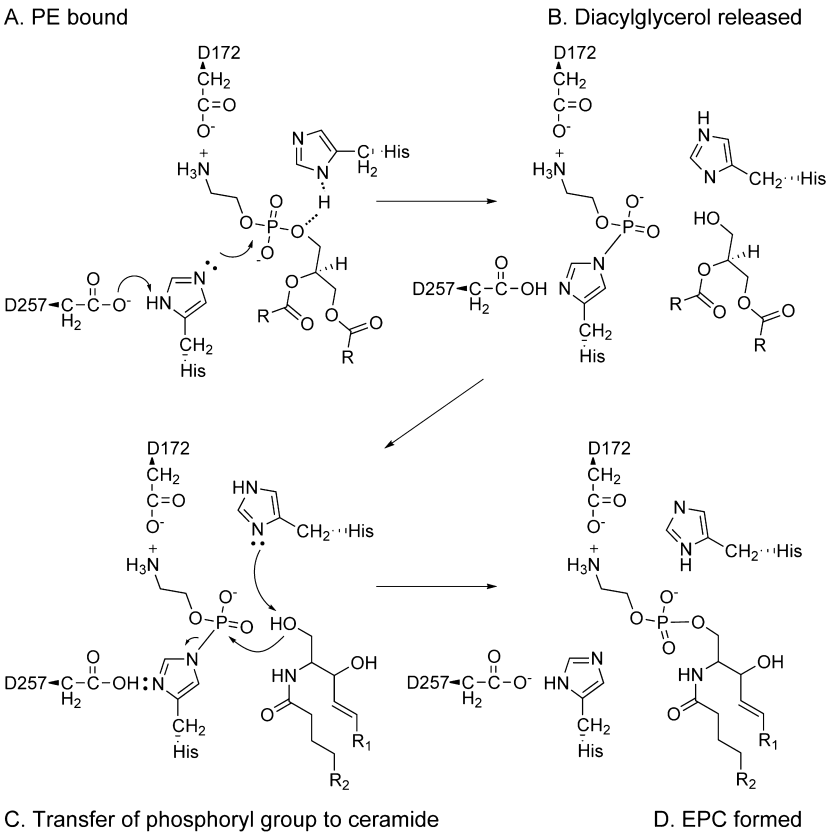

Figure 7. Reaction mechanism proposed for TbSLS3. (A) Binding of PE is oriented by interaction of the substrate primary amine group with the carboxylate group of D172. (B) Displacement of diacylglycerol is promoted by acid–base catalysis provided by the conserved HHD triad. (C) Binding of ceramide and nucleophilic attack of the hydroxyl group with activation by acid–base catalysis. The NBD moiety of NBD-C6-CM would be located three methylene groups beyond R2, so is located distal from the active site. (D) Formation of EPC.

approach for functional characterization is applicable to these proteins as well.

Evolutionary Implications of Trypanosomatid SLS Genomic Organization of Genes. All of the trypanosomatid SLS loci reside in syntenic chromosomal locations, confirming the evolutionary relatedness of the clade (Figure 6B). There is a striking amplification and diversification of SLS genes and activities within the *T. brucei* ssp that is not seen in *T. vivax*, which diverges at the root of the African trypanosome lineage.[36] The fact that the outlying *T. cruzi* and *L. major* genomes have single SLSs encoding exclusive IPC synthase activities suggests that this is the ancestral genotype within the entire trypansomatid clade. The sequence alignment (Figure 6A) does not allow confident in silico prediction of TvSLS1 activity, as the presence of tyrosine at position 252 could be consistent with either IPC (S252, hydroxylated) or SM/EPC (Phe252, bulky hydrophobic) activities. Resolution of this issue will have implications for the evolutionary biology of the African trypanosomes. Of all the trypanosomatid parasites of mammals, the replicative form in the mammalian host is entirely extracellular in only the African lineage. The *Leishmanias* and *T. cruzi* all replicate intracellularly. Perhaps the ability to synthesize mammalian type sphingolipids was a critical adaptation to life in the mammalian bloodstream. Conversely, retention of the capacity to synthesize IPC may be critical for life in the various insect vectors that are central to transmission of each of these parasites. This would be consistent with the fact that IPC synthesis is developmentally up-regulated in the insect stage of the *T. b. brucei* life cycle. On the basis of these considerations, it might then be predicted that the *T. vivax* SLS is a multifunctional enzyme capable of synthesizing both IPC and the zwitterionic sphingolipids, which allowed subsequent duplication and specialization of SLS activities in the more recently derived *T. brucei* ssp.

Homology Models of the PAP2 Superfamily Active Site. The SLS enzymes are part of the PAP2 superfamily (PFAM Pf05169) along with lipid phosphate phosphatase,[37] glucose-6-phosphatase,[38,39] fungal haloperoxidases,[40] and others.[13] The presence of a phosphatase motif in *Curvularia inaequalis* chloroperoxidase, and the crystal structure (PDB ID 1IDQ[41]) showing the coordination of H496 NE2 to VO_4^{3-}, the hydrogen-bonding interaction between D500 and H496 ND1, and the hydrogen-bonding interaction of H404 ND1 were used to define the core properties of an active site utilizing the HHD motif. Additional detailed inferences about the nature of the active sites are less certain because of the low sequence identity between the integral membrane members of the superfamily and the few soluble members whose structures are known. For example, recent homology model calculations (http://www.proteinmodelportal.org/) suggest that glucose-6-phosphatase is best modeled by the PAP2 superfamily member *Salmonella typhimurium* PhoN (PDB ID 1d2t[42]), but the estimated coordinate position error for atoms in the modeled structure is ~12 Å. Similar large coordinate errors are associated with models of mammalian glucose-6-phosphatase obtained using chloroperoxidase as the structure template (PDB ID 1IDQ).

Homology modeling of the trypanosomal SLS paralogs has also been undertaken, and the results are publically available at

the Protein Structure Initiative Structural Biology Knowledge-Base Protein Model Portal (http://www.proteinmodelportal.org/). In summary, PSI-BLAST returned no suitable matches between any of the TbSLS primary sequences and solved structures in the PDB, and no reasonable homology models for TbSLS3 and TbSLS4 have been calculated. Furthermore, 264 of 355 residues of TbSLS1 were modeled to the template cytochrome *c* oxidase (PDB ID 1M56) with ~10 Å coordinate error and 184 of 272 residues of TbSLS2 were modeled to the WO_4^{2-} complex of PhoN (PDB ID 2akc) with ~15 Å coordinate error. Clearly, these results highlight the uncertainties inherent in modeling structures with low identity of primary sequence and also emphasize the need for experimental studies to confirm hypotheses regarding active site structure and enzymatic function.

Active Site Triad and Proposed Mechanism. Figure 7A shows a reaction mechanism for TbSLS3 consistent with the biochemical studies presented here and other contributions. This work suggests a role for participation of the HHD triad as general acid/base catalysts in the SLS reaction and also indicates other residues that provide the observed substrate selectivity. As discussed elsewhere,[10] the SLS reaction is likely ordered, proceeding with binding of the donor substrate (PE in the case of the TbSLS3 reaction shown in Figure 7A), possibly formation of a phosphorylhistidine adduct like that detected in glucose-6-phosphatase[39] and suggested by the crystal structure of chloroperoxidase complexed with VO_4^{3-}.[41] In accord with this structure, the role of D257 would be to activate H253 for nucleophilic attack on the phosphoryl group of the initial substrate. As the elimination of DAG is often assisted by general acid catalysis, the role of the other His of the HHD triad may to catalyze this elimination (Figure 7B). The positioning of H210 may allow it to also participate in the activation of CM during the second part of the reaction (Figure 7B). After transfer of the phosphoryl group from the enzyme to the acceptor, release of the product (EPC in this case) would complete the reaction.

For TbSLS3 and TbSLS4, binding of PE would be stabilized by electrostatic interactions between the protonated amine group of substrate and the carboxylate group of D172 (Figure 7A, step 1). A similar charge pairing may stabilize the binding of PC in the bifunctional active sites of TbSLS3 and TbSLS4. For IPC synthesis, no charged residue was identified to be required. Instead, steric interactions and possibly hydrogen-bonding interactions impart the catalytic selectivity.

Alternatively, acyl phosphate intermediates are proposed in a number of enzyme reactions.[43−52] In principle, the Asp residue of the HHD might also serve as a nucleophile at the start of the reaction and thus generate a phosphoacyl intermediate. In this alternative, the role of the His residues would be to provide activation of the incoming phosphoryl group, assist with DAG as a leaving group, and activate of the acceptor hydroxyl group on CM. Further experimental tests of these mechanistic options are possible using purified preparations of the integral membrane enzymes provided by the cell-free translation method.

■ ASSOCIATED CONTENT

Ⓢ Supporting Information

Mutagenic primers (Table S1), primary sequence alignments of *T. brucei* SLS paralogs (Figure S1), single mutation analysis of *T. brucei* SLS2 and SLS4 and consequences on product distributions (Figure S2), and reciprocal mutations of *T. brucei* SLS2 and SLS4 leading to interconversion between EPC and SM/EPC reactions (Figure S2). This material is available free of charge via the Internet at http://pubs.acs.org.

■ AUTHOR INFORMATION

Corresponding Author

*Tel 608 262-9708, e-mail bgfox@biochem.wisc.edu (B.G.F.); tel 608-262-3110, e-mail jdbangs@wisc.edu (J.D.B.).

Present Address

⊥Department of Biochemistry, Weill Cornell Medical College, 1300 York Avenue, New York, NY 10065.

■ ACKNOWLEDGMENTS

United States Public Health Service Grants NIAID R01 AI35739 to J.D.B. and National Institutes of General Medical Sciences Protein Structure Initiative Grant 1 U54 GM074901 to B.G.F. supported this work.

■ REFERENCES

(1) Schuck, S., and Simons, K. (2004) Polarized sorting in epithelial cells: raft clustering and the biogenesis of the apical membrane. *J. Cell Sci. 117*, 5955−5964.

(2) Lahiri, S., and Futerman, A. H. (2007) The metabolism and function of sphingolipids and glycosphingolipids. *Cell. Mol. Life Sci. 64*, 2270−2284.

(3) Zhang, K., Pompey, J. M., Hsu, F. F., Key, P., Bandhuvula, P., Saba, J. D., Turk, J., and Beverley, S. M. (2007) Redirection of sphingolipid metabolism toward de novo synthesis of ethanolamine in Leishmania. *EMBO J. 26*, 1094−1104.

(4) Lingwood, D., and Simons, K. (2010) Lipid rafts as a membrane-organizing principle. *Science 327*, 46−50.

(5) Simons, K., and Gerl, M. J. (2010) Revitalizing membrane rafts: new tools and insights. *Nat. Rev. Mol. Cell Biol. 11*, 688−699.

(6) Brindley, D. N., and Waggoner, D. W. (1998) Mammalian lipid phosphate phosphohydrolases. *J. Biol. Chem. 273*, 24281−24284.

(7) Huitema, K., van den Dikkenberg, J., Brouwers, J. F., and Holthuis, J. C. (2004) Identification of a family of animal sphingomyelin synthases. *EMBO J. 23*, 33−44.

(8) Tafesse, F. G., Huitema, K., Hermansson, M., van der Poel, S., van den Dikkenberg, J., Uphoff, A., Somerharju, P., and Holthuis, J. C. (2007) Both sphingomyelin synthases SMS1 and SMS2 are required for sphingomyelin homeostasis and growth in human HeLa cells. *J. Biol. Chem. 282*, 17537−17547.

(9) van Meer, G., and Holthuis, J. C. (2000) Sphingolipid transport in eukaryotic cells. *Biochim. Biophys. Acta 1486*, 145−170.

(10) Tafesse, F. G., Ternes, P., and Holthuis, J. C. (2006) The multigenic sphingomyelin synthase family. *J. Biol. Chem. 281*, 29421−29425.

(11) Serricchio, M., and Butikofer, P. (2011) Trypanosoma brucei: a model micro-organism to study eukaryotic phospholipid biosynthesis. *FEBS J 278*, 1035−1046.

(12) Sutterwala, S. S., Hsu, F. F., Sevova, E. S., Schwartz, K. J., Zhang, K., Key, P., Turk, J., Beverley, S. M., and Bangs, J. D. (2008) Developmentally regulated sphingolipid synthesis in African trypanosomes. *Mol. Microbiol. 70*, 281−296.

(13) Stukey, J., and Carman, G. M. (1997) Identification of a novel phosphatase sequence motif. *Protein Sci. 6*, 469−472.

(14) Ternes, P., Brouwers, J. F., van den Dikkenberg, J., and Holthuis, J. C. (2009) Sphingomyelin synthase SMS2 displays dual activity as ceramide phosphoethanolamine synthase. *J. Lipid Res. 50*, 2270−2277.

(15) Levine, T. P., Wiggins, C. A., and Munro, S. (2000) Inositol phosphorylceramide synthase is located in the Golgi apparatus of *Saccharomyces cerevisiae*. *Mol. Biol. Cell 11*, 2267−2281.

(16) Neuwald, A. F. (1997) An unexpected structural relationship between integral membrane phosphatases and soluble haloperoxidases. *Protein Sci. 6*, 1764−1767.

(17) Hemrika, W., Renirie, R., Dekker, H. L., Barnett, P., and Wever, R. (1997) From phosphatases to vanadium peroxidases: a similar architecture of the active site. *Proc. Natl. Acad. Sci. U. S. A. 94*, 2145−2149.

(18) Zhang, Q. X., Pilquil, C. S., Dewald, J., Berthiaume, L. G., and Brindley, D. N. (2000) Identification of structurally important domains of lipid phosphate phosphatase-1: implications for its sites of action. *Biochem. J. 345* (Pt 2), 181−184.
(19) Pan, C. J., Lei, K. J., Annabi, B., Hemrika, W., and Chou, J. Y. (1998) Transmembrane topology of glucose-6-phosphatase. *J. Biol. Chem. 273*, 6144−6148.
(20) Jasinska, R., Zhang, Q. X., Pilquil, C., Singh, I., Xu, J., Dewald, J., Dillon, D. A., Berthiaume, L. G., Carman, G. M., Waggoner, D. W., and Brindley, D. N. (1999) Lipid phosphate phosphohydrolase-1 degrades exogenous glycerolipid and sphingolipid phosphate esters. *Biochem. J. 340* (Pt 3), 677−686.
(21) Vacaru, A.M., Tafesse, F. G., Ternes, P., Kondylis, V., Hermansson, M., Brouwers, J. F., Somerharju, P., Rabouille, C., and Holthuis, J. C. (2009) Sphingomyelin synthase-related protein SMSr controls ceramide homeostasis in the ER. *J. Cell Biol. 185*, 1013−1027.
(22) Neuwald, A. F. (1997) An unexpected structural relationship between integral membrane phosphatases and soluble haloperoxidases. *Protein Sci. 6*, 1764−1767.
(23) Yeang, C., Varshney, S., Wang, R., Zhang, Y., Ye, D., and Jiang, X. C. (2008) The domain responsible for sphingomyelin synthase (SMS) activity. *Biochim. Biophys. Acta 1781*, 610−617.
(24) Sevova, E. S., Goren, M. A., Schwartz, K. J., Hsu, F. F., Turk, J., Fox, B. G., and Bangs, J. D. (2010) Cell-free synthesis and functional characterization of sphingolipid synthases from parasitic trypanosomatid protozoa. *J. Biol. Chem. 285*, 20580−20587.
(25) Zhang, K., Bangs, J. D., and Beverley, S. M. (2010) Sphingolipids in parasitic protozoa. *Adv. Exp. Med. Biol. 688*, 238−248.
(26) Goren, M. A., and Fox, B. G. (2008) Wheat germ cell-free translation, purification, and assembly of a functional human stearoyl-CoA desaturase complex. *Protein Expression Purif. 62*, 171−178.
(27) Blommel, P. G., Martin, P. A., Wrobel, R. L., Steffen, E., and Fox, B. G. (2006) High efficiency single step production of expression plasmids from cDNA clones using the Flexi Vector cloning system. *Protein Expression Purif. 47*, 562−570.
(28) Sawasaki, T., Hasegawa, Y., Tsuchimochi, M., Kasahara, Y., and Endo, Y. (2000) Construction of an efficient expression vector for coupled transcription/translation in a wheat germ cell-free system. *Nucleic Acids Symp. Ser.*, 9−10.
(29) Goren, M. A., Nozawa, A., Makino, S., Wrobel, R. L., and Fox, B. G. (2009) Cell-free translation of integral membrane proteins into unilamellar liposomes. *Methods Enzymol. 463*, 647−673.
(30) Martin, O. C., and Pagano, R. E. (1994) Internalization and sorting of a fluorescent analogue of glucosylceramide to the Golgi apparatus of human skin fibroblasts: utilization of endocytic and nonendocytic transport mechanisms. *J. Cell Biol. 125*, 769−781.
(31) O'Donovan, C., and Apweiler, R. (2011) A guide to UniProt for protein scientists. *Methods Mol. Biol. 694*, 25−35.
(32) Thompson, J. D., Higgins, D. G., and Gibson, T. J. (1994) CLUSTAL W: improving the sensitivity of progressive multiple sequence alignment through sequence weighting, position-specific gap penalties and weight matrix choice. *Nucleic Acids Res. 22*, 4673−4680.
(33) Arnold, K., Kiefer, F., Kopp, J., Battey, J. N., Podvinec, M., Westbrook, J. D., Berman, H. M., Bordoli, L., and Schwede, T. (2009) The Protein Model Portal. *J. Struct. Funct. Genomics 10*, 1−8.
(34) Denny, P. W., Shams-Eldin, H., Price, H. P., Smith, D. F., and Schwarz, R. T. (2006) The protozoan inositol phosphorylceramide synthase: a novel drug target which defines a new class of sphingolipid synthase. *J. Biol. Chem. 281*, 28200−28209.
(35) Aslett, M., Aurrecoechea, C., Berriman, M., Brestelli, J., Brunk, B. P., Carrington, M., Depledge, D. P., Fischer, S., Gajria, B., Gao, X., Gardner, M. J., Gingle, A., Grant, G., Harb, O. S., Heiges, M., Hertz-Fowler, C., Houston, R., Innamorato, F., Iodice, J., Kissinger, J. C., Kraemer, E., Li, W., Logan, F. J., Miller, J. A., Mitra, S., Myler, P. J., Nayak, V., Pennington, C., Phan, I., Pinney, D. F., Ramasamy, G., Rogers, M. B., Roos, D. S., Ross, C., Sivam, D., Smith, D. F., Srinivasamoorthy, G., Stoeckert, C. J. Jr., Subramanian, S., Thibodeau, R., Tivey, A., Treatman, C., Velarde, G., and Wang, H. (2010) TriTrypDB: a functional genomic resource for the Trypanosomatidae. *Nucleic Acids Res. 38*, D457−462.
(36) Hamilton, P. B., Gibson, W. C., and Stevens, J. R. (2007) Patterns of co-evolution between trypanosomes and their hosts deduced from ribosomal RNA and protein-coding gene phylogenies. *Mol. Phylogenet. Evol. 44*, 15−25.
(37) Waggoner, D. W., Xu, J., Singh, I., Jasinska, R., Zhang, Q. X., and Brindley, D. N. (1999) Structural organization of mammalian lipid phosphate phosphatases: implications for signal transduction. *Biochim. Biophys. Acta 1439*, 299−316.
(38) Hemrika, W., and Wever, R. (1997) A new model for the membrane topology of glucose-6-phosphatase: the enzyme involved in von Gierke disease. *FEBS Lett. 409*, 317−319.
(39) Ghosh, A., Shieh, J. J., Pan, C. J., and Chou, J. Y. (2004) Histidine 167 is the phosphate acceptor in glucose-6-phosphatase-beta forming a phosphohistidine enzyme intermediate during catalysis. *J. Biol. Chem. 279*, 12479−12483.
(40) Macedo-Ribeiro, S., Hemrika, W., Renirie, R., Wever, R., and Messerschmidt, A. (1999) X-ray crystal structures of active site mutants of the vanadium-containing chloroperoxidase from the fungus Curvularia inaequalis. *JBIC, J. Biol. Inorg. Chem. 4*, 209−219.
(41) Messerschmidt, A., Prade, L., and Wever, R. (1997) Implications for the catalytic mechanism of the vanadium-containing enzyme chloroperoxidase from the fungus Curvularia inaequalis by X-ray structures of the native and peroxide form. *Biol. Chem. 378*, 309−315.
(42) Ishikawa, K., Mihara, Y., Gondoh, K., Suzuki, E., and Asano, Y. (2000) X-ray structures of a novel acid phosphatase from Escherichia blattae and its complex with the transition-state analog molybdate. *EMBO J. 19*, 2412−2423.
(43) Stelte, B., and Witzel, H. (1986) Formation of an aspartyl phosphate intermediate in the reactions of nucleoside phosphotransferase from carrots. *Eur. J. Biochem. 155*, 121−124.
(44) Sanders, D. A., Gillece-Castro, B. L., Stock, A. M., Burlingame, A. L., and Koshland, D. E. Jr. (1989) Identification of the site of phosphorylation of the chemotaxis response regulator protein, CheY. *J. Biol. Chem. 264*, 21770−21778.
(45) Collet, J. F., Stroobant, V., Pirard, M., Delpierre, G., and Van Schaftingen, E. (1998) A new class of phosphotransferases phosphorylated on an aspartate residue in an amino-terminal DXDX(T/V) motif. *J. Biol. Chem. 273*, 14107−14112.
(46) Goudreau, P. N., Lee, P. J., and Stock, A. M. (1998) Stabilization of the phospho-aspartyl residue in a two-component signal transduction system in Thermotoga maritima. *Biochemistry 37*, 14575−14584.
(47) Pirard, M., Achouri, Y., Collet, J. F., Schollen, E., Matthijs, G., and Van Schaftingen, E. (1999) Kinetic properties and tissular distribution of mammalian phosphomannomutase isozymes. *Biochem. J. 339* (Pt 1), 201−207.
(48) Napper, S., Delbaere, L. T., and Waygood, E. B. (1999) The aspartyl replacement of the active site histidine in histidine-containing protein, HPr, of the Escherichia coli Phosphoenolpyruvate:Sugar phosphotransferase system can accept and donate a phosphoryl group. Spontaneous dephosphorylation of acyl-phosphate autocatalyzes an internal cyclization. *J. Biol. Chem. 274*, 21776−21782.
(49) Allegrini, S., Scaloni, A., Ferrara, L., Pesi, R., Pinna, P., Sgarrella, F., Camici, M., Eriksson, S., and Tozzi, M. G. (2001) Bovine cytosolic 5′-nucleotidase acts through the formation of an aspartate 52-phosphoenzyme intermediate. *J. Biol. Chem. 276*, 33526−33532.
(50) McIntosh, D. B., Montigny, C., and Champeil, P. (2008) Unexpected phosphoryl transfer from Asp351 to fluorescein attached to Lys515 in sarcoplasmic reticulum Ca2+-ATPase. *Biochemistry 47*, 6386−6393.
(51) Lahiri, S. D., Zhang, G., Dunaway-Mariano, D., and Allen, K. N. (2003) The pentacovalent phosphorus intermediate of a phosphoryl transfer reaction. *Science 299*, 2067−2071.
(52) Zhang, Y. M., and Rock, C. O. (2008) Thematic review series: Glycerolipids. Acyltransferases in bacterial glycerophospholipid synthesis. *J. Lipid Res. 49*, 1867−1874.